



PCCP

**Investigation of the Stability of D5SIC-DNAM-Incorporated
DNA duplex in Taq Polymerase Binary system: A Systematic
Classical MD Approach**

Journal:	<i>Physical Chemistry Chemical Physics</i>
Manuscript ID	CP-ART-11-2023-005571.R1
Article Type:	Paper
Date Submitted by the Author:	29-Jan-2024
Complete List of Authors:	Debnath, Tanay; The University of Texas at Dallas, Physics Cisneros, Andres; The University of Texas at Dallas, Physics

SCHOLARONE™
Manuscripts

ARTICLE

Investigation of the Stability of D5SIC-DNAM-Incorporated DNA duplex in *Taq* Polymerase Binary system: A Systematic Classical MD Approach

Tanay Debnath^a, G. Andres Cisneros^{a,b*}

DNA polymerases are fundamental enzymes that play a crucial role in processing DNA with high fidelity and accuracy ensuring the faithful transmission of genetic information. The recognition of unnatural base pairs (UBPs) by polymerases, enabling their replication, represents a significant and groundbreaking discovery with profound implications for genetic expansion. Romesberg et al. examined the impact of DNA containing 2,6-dimethyl-2H-isoquinoline-1-thione: D5SIC (DS) and 2-methoxy-3-methylnaphthalene: DNAM (DN) UBPs bound to *T. aquaticus* DNA polymerase (*Taq*) through crystal structure analysis. Here, we have used polarizable and nonpolarizable classical molecular dynamics (MD) simulations to investigate the structural aspects and stability of *Taq* in complex with a DNA duplex including a DS-DN pair in the terminal 3' and 5' positions. Our results suggest that the flexibility of UBP-incorporated DNA in the terminal position is arrested by the polymerase, thus preventing fraying and mispairing. Our investigation also reveals that the UBP remains in an intercalated conformation inside the active site, exhibiting two distinct orientations in agreement with experimental findings. Our analysis pinpoints particular residues responsible for favorable interactions with the UBP, with some relying on van der Waals interactions while other on Coulombic forces.

Introduction

The precise synthesis and repair of DNA¹ within cells relies extensively on a complex network of proteins of which DNA polymerases are key players.²⁻⁵ In biological process, DNA polymerases are specific towards four nucleotides (A, T, G, C) and two base-pairings (A-T and G-C).¹⁻⁶ The concept of incorporating synthetic molecules as base pairs, termed Unnatural Base-Pairs (UBPs)⁷⁻⁴², depends upon a crucial prerequisite: these synthetic entities must undergo a thorough selection process orchestrated by polymerase enzymes.⁴³⁻⁵⁰ In essence, the viability of these synthetic molecules as base pairs is contingent upon the polymerase's ability to discriminate and incorporate them into the growing DNA strand with a high degree of accuracy and efficiency. This selectivity is essential to ensure that the resulting DNA sequence maintains fidelity and stability, akin to the natural base pairs (nBPs), and to avoid introducing errors or disruptions that could compromise the biological function of

DNA. As a result, successful recognition and incorporation of unnatural bases by DNA polymerases is fundamental to their potential utilization in various biotechnological and genetic engineering applications.

Several potential UBPs have been synthesized in recent years³⁰⁻⁴² among them d5SICS (DS)-dNaM (DN) have emerged as one of the proficiently replicated unnatural base pairs.³⁰⁻³¹ Previous reported work revealed that DS-DN form unconventional structures inside a DNA duplex. Bertz *et al.* reported two crystal structures of a DNA polymerase in complex with DNA containing a DS-DN incorporation^{30,31}. The first report involves a crystal structure of DNA polymerase I from *T. aquaticus* (*Taq*) in a closed ternary complex with DN in the templating position, and DS- triphosphate (DSTP) as substrate (PDB ID :3SV3).³⁰ In this structure, DN and DSTP exhibit Watson-Crick-Franklin (WCF) like parallelly stacked geometry.

Later they also reported the binary complex of *Taq* with the artificial base pair DS-DN in the post-insertion site. Crystal structures showed that in the binary complex of the polymerase, DS-DN forms two distinct intercalated non-Watson-Crick-Franklin (nWCF) structures in the terminal position of the DNA duplex. In one structure (PDB ID: 4C8L)³¹, the primer-DS is located externally with respect to the

^a Department of Physics, University of Texas at Dallas, Richardson, TX, Dallas, USA.

^b Department of Chemistry and Biochemistry, University of Texas at Dallas, Richardson, TX, Dallas, USA.

Electronic Supplementary Information (ESI) available: Additional details of MD, EDA (PDF)

Additional ESI for the initial coordinates and parameters for all of the studied systems (ESI-1.zip) (ZIP)

NMA movies of all the conformers (NMA.zip) (ZIP)

substrate-DS; whereas in another (PDB ID: 4C80)³¹ the positioning becomes opposite.

Different computational techniques have been employed to predict the impact of DS-DN inside DNA in aqueous solvent, which predict both WCF and nWCF structures of the UBP inside DNA without polymerase systems.⁵¹⁻⁵⁸ Our previous theoretical work⁵¹ suggests that the inclusion of a DS-DN pair at the terminal position of DNA increases the flexibility of these bases, with occasional mispairing and fraying.

Romesberg *et. al* further reported individual residue contacts between *Taq* and the UBP-incorporated DNA based on the X-ray crystal structures.³¹ Although this investigation provided valuable insights into possible molecular interactions, a comprehensive interplay between *Taq* and UBP-incorporated-DNA including their dynamic characteristics, remains a subject yet to be thoroughly investigated. The full scope of how a polymerase orchestrates the interactions, and the dynamic nature of these connections remains an unsolved avenue for further exploration and scientific inquiry.

Here, we have employed classical molecular dynamics simulation with both AMOEBA and AMBER force fields to investigate the dynamical characteristics of UBP-incorporated DNA in binary complex with *Taq* and the molecular level interactions of UBP incorporated DNA with *Taq*. The remainder of the paper is organized as follows: The next section describes the setup of the simulation systems, simulation procedures, and analyses. Subsequently, analysis of the MD simulations is presented and discussed, followed by concluding remarks. This work is intended to provide novel insights on the DNA polymerase-bound behaviour of DNA that incorporates an experimentally synthesized and tested UBP that can be replicated, translated and transcribed *in vitro*. Our results uncover the specific drivers for the stabilization and selectivity of specific pairing of the UBP in the active site, which can help drive the field of synthetic biology forward.

Computational Methods

System Setup

We have considered two types of binary complexes of *Taq* with a DS-DN UBP in the post-insertion site. In one case PDB ID: 4C8L has been used to generate a model where DS is externally placed with respect to DN designated as EXT. Additionally, the INT structure has been generated by using the PDB ID: 4C80 crystal structure where DS is placed below DN (Figure 1). These EXT and INT structures are linked through the inter-strand flipping process of the UBP. In both cases the UBP adopts an intercalated configuration with the sulfur and methoxy groups in the same phase (SYN). We have also considered ANTI structures for both EXT and INT where the sulfur and methoxy groups are on opposite sides. All

together four structures have been considered: EXT_{SYN}, EXT_{ANTI}, INT_{SYN}, INT_{ANTI}. Both the EXT_{SYN} and INT_{SYN} have been simulated in two ways; i) UBP-incorporated DNA with one single overhang base and ii) truncated UBP-incorporated DNA. We have considered one single orientation of the glycosidic bond as reported in the crystal structures. The *Taq* fragment consists of 541 amino acid residues with residue numbers from 292 to 832. The residue numbers of DNA base-pairs are from 833 to 855 with DS and DN located in positions 843 and 846 respectively. The distance between DS and DN is

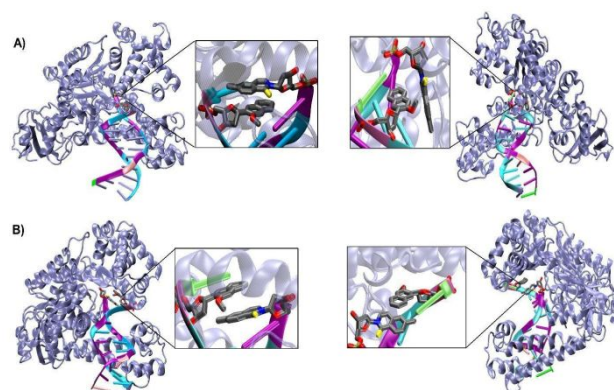


Figure 1. Binary complex of *Taq* with the artificial base pair DS-DN where A) DS is externally intercalated, EXT_{SYN} (left) and EXT_{ANTI} (right) B) DS is internally placed with respect to DN; INT_{SYN} (left) and INT_{ANTI} (right).

designated as $d_{\text{DS-DN}}$. The distance between the UB and its adjacent NB is designated as $d_{\text{DS-DC}}$ and $d_{\text{DN-DG}}$ respectively. The $\langle \text{DS-P-DC} \rangle$ and $\langle \text{DN-P-DG} \rangle$ have been also calculated as depicted in Figure S1. Parameters for the DS and DN bases were obtained with the PYRED program⁵⁹ for AMBER⁶⁰⁻⁶². For the required AMOEBA parameters⁶³⁻⁶⁶ we have used TINKER⁶⁷ and GDMA 2.3⁶⁸. All new parameters are included as electronic supplementary information (SI).

AMBER Setup

The LEaP module⁶⁹ in AMBER20⁷⁰ was used to set up the simulation box with *Taq* with UBP-incorporated DNA systems. The PROPKA software is adopted to protonate the amino acids of the *Taq*.^{71, 72} Adding the hydrogen atoms to the systems, neutralization of the system with the required number of counterions (Na^+), and solvation of the system in a cubic box filled with TIP3P water⁶⁰, extending at least 12 Å from the Protein-DNA complex was done with the LEaP module from AMBER. The MD simulations were performed via AMBER20 pmemd.cuda using ff14SB AMBER force field⁶¹ for protein OL15 for nucleic acid⁶². Seven minimization steps were done with decreasing restraint ($10.0-0.0 \text{ kcal mol}^{-1} \text{ \AA}^{-2}$) on the solute's heavy atoms. In each stage, the system was minimized within 5000 cycles of minimization via the steepest descent algorithm, continuing with 5000 cycles via the conjugated

gradient algorithm. In the next step, each system was heated to 300 K using Langevin dynamics with a collision frequency of 2 ps^{-1} followed by 7 ns of NVT equilibration with decreasing restraint ($10.0\text{--}0.0 \text{ kcal mol}^{-1} \text{ \AA}^{-2}$) on the protein's heavy atoms. The production calculations for each system were accomplished in 250 ns of NPT ensemble without restraints in triplicate for a total of 750 ns of production simulation for each system. Production was run in the NPT ensemble using a Langevin thermostat and Berendsen barostat. Temperature was held constant at 300 K and pressure at 1.0 bar with a 2 fs time step. The SHAKE method⁷³ has been employed for the bonds with hydrogen atoms, and for long-range Coulomb interactions, the smooth particle mesh Ewald approach⁷⁴ was used with a 10 Å cutoff for nonbonded interactions. The CPPTRAJ module⁷⁵ in AMBER20 was used to analyze production dynamics, i.e., RMSD, RMSF, correlation, normal mode analysis and geometrical parameters. In addition, Python libraries NumPy⁷⁶, Matplotlib⁷⁷, Pandas⁷⁸, were also employed for further data processing and graphing. A total of 12500 frames have been extracted from the entire trajectory of each replicate for the analysis. Energy decomposition analysis (EDA) has been employed to investigate the intermolecular interactions between the UBP and residues of the rest of the systems for the entire trajectory using 12500 frames for two replicates. As both the replicates show similar outcomes, the rest of the analysis has been done for one replicate. Amber-EDA was employed to calculate the nonbonded intermolecular interaction energies⁷⁹.

AMOEBA Setup

All polarizable AMOEBA (Atomic Multipole Optimized Energetics for Biomolecular)⁶³⁻⁶⁶ simulations were performed with TINKER-HP⁶⁷. The simulation box with the protein-DNA system was built with the help of packmol software.⁸⁰ Initially, the *Taq* and UBP-incorporated DNA duplex complex was minimized using the BFGS nonlinear optimization algorithm with a convergence criterion (RMS gradient) of 0.1 Å. Subsequently molecular dynamics simulations in vacuum followed by implicit water with the GBSA model for 2 ns were carried out to relax the system. The resulting system was solvated using 72000 AMOEBA water molecules and neutralized using Na^+ in the center of the box with volume $90 \times 90 \times 90 \text{ \AA}^3$ using packmol. After that, the system was heated to 300 K in 4 simulation steps (2 ns each) with an NVT ensemble removing all positional restraints ($100.0\text{--}0.0 \text{ kcal/ \AA}^{-1}$). After the equilibration step, MD simulations were carried out for 50 ns in an NPT ensemble (1 atm and 300 K). The Monte Carlo barostat and the Bussi thermostat were used to keep the pressure and temperature fixed respectively. The

duration of the time step was 2 fs using RESPA integrator. The smooth particle mesh Ewald (sPME) method⁸¹ was used in the calculation of charge, atomic multipole, and polarization interactions. A value of 10 Å was used for the cutoff distance value for van der Waals potential energy interactions and the real-space distance cutoff in the Ewald summation.⁸² Geometry sampling was done every 5 ps, which led to generate total 10000 frames.

Results and Discussion

The results for the EXT_{SYN} conformer systems (Figure 1) simulated using the AMBER force field suggest that the DS-DN pair maintains an intercalated orientation in the DNA duplex for the entire 250 ns duration in all three replicates. No deviation from the intercalated structure of the DS-DN pair inside the DNA duplex were observed from the simulation with AMOEBA force field for 50ns in two replicates. The low RMSD value (Table 1 and Figure S2) suggests that the system is stable throughout the simulation. This indicates that the flexibility of the UBP in DNA observed in aqueous solution as previously reported⁵¹ is arrested by the polymerase, which is also consistent with the per-residue RMSF values (Figure 3).

Table 1. Average RMSD values and standard deviation of RMSD values of each replicate of each system obtained from AMOEBA and AMBER simulations. The values are in Å.

	RMSD/STDV		
	Rep1	Rep2	Rep3
	AMOEBA		
EXT_{SYN}	2.71/0.37	1.56/0.23	
INT_{SYN}	2.17/0.29	2.23/0.24	
	AMBER		
EXT_{SYN}	2.11/0.26	2.40/0.28	2.21/0.30
INT_{SYN}	2.58/0.30	2.40/0.31	2.58/0.41
INT_{ANTI}	2.65/0.40	2.29/0.23	2.72/0.46
EXT_{ANTI}	2.87/0.40	2.93/0.39	2.79/0.45

Table 2. Average DS-DN distance and standard deviation of RMSD values of each replicate of each system obtained from AMOEBA and AMBER simulations. The values are in Å. In Crystal structure DS-DN of EXT_{SYN} is 8.44 Å and INT_{SYN} is 9.36 Å.

	Distance/STDV		
	Rep1	Rep2	Rep3
	AMOEBA		
EXT_{SYN}	8.08/0.45	8.10/0.38	
INT_{SYN}	9.10/0.32	7.52/0.62	
	AMBER		
EXT_{SYN}	8.60/0.77	8.86/0.87	7.89/1.13
INT_{SYN}	9.63/0.44	9.67/0.47	9.71/0.38
INT_{ANTI}	9.06/0.73	9.07/0.76	9.19/0.86

The distance between DS and DN ($d_{\text{DS-DN}}$) (Table 2 and Figure S3) based on both AMOEBA and AMBER simulation, indicating a reduced distance compared to that of a nBP of ~ 10.5 Å. We have also measured the distance (Figure 2) and angles (Figure S4) of UBPs with respect to their adjacent nBP. It has been found that throughout the simulation the gap between $d_{\text{DS-DC}}$ and $d_{\text{DN-DG}}$ is always positive indicating the asymmetric nature of the DNA strand with external intercalation of DS and DN (Figure 2). From angle analysis the asymmetric nature of DNA is also observed since $\langle \text{DS-P-DC} \rangle$ is found to be greater than $\langle \text{DN-P-DG} \rangle$ throughout entire trajectory of the simulation. In the crystal structure a similar trend for the UB-NB and $\langle \text{UB-P-NB} \rangle$ have been observed.

Similar to AMBER, simulations with the AMOEBA force field for 50 ns for EXT_{SYN} also result in an intercalated DS-DN structure with no conformational change and no significant distortion inside the polymerase. Here also, the DS-DN distance is found to be shorter than that of nBPs. AMOEBA also predicts greater $d_{\text{DS-DC}}$ and $\langle \text{DS-P-DC} \rangle$ than $d_{\text{DN-DG}}$ and $\langle \text{DN-P-DG} \rangle$ (Figure 2 and Figure S4) and throughout the simulations supporting an external intercalation of the UBP leading to the maintenance of an asymmetric DNA strand structure. From the AMBER and AMOEBA simulations, it becomes apparent that both yield mostly similar results in terms of RMSD values and related geometric parameters. Furthermore, the simulations show minimal deviations from the actual crystal structures, suggesting that the molecular dynamics (MD) simulations align closely with the experimental observation of binary *Taq*

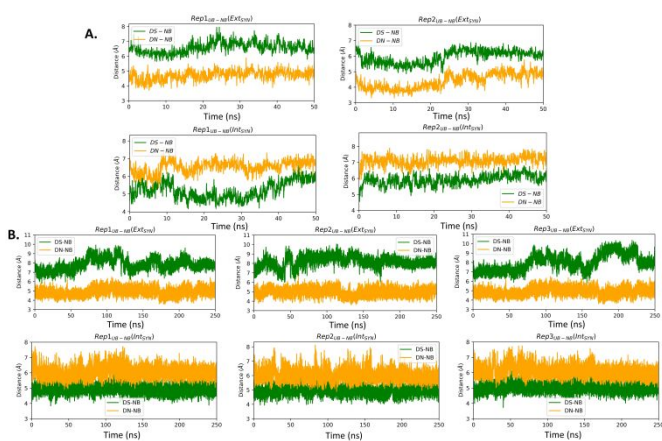


Figure 2. UB-NB distances obtained from A) AMOEBA and B) AMBER force field-mediated simulations. In crystal structure, DS-DC and DN-DG is 6.69 Å and 4.64 Å respectively for EXT_{SYN} and 4.98 Å and 6.04 Å respectively for INT_{SYN} .

with UBP-incorporated DNA. Interestingly, with no-overhang DNA, the simulation with AMBER also predicts similar stability and structural features indicating an overhanging

base doesn't significantly impact UBP stability when the dsDNA is in complex with *Taq*. The associated RMSD, RMSF and geometrical parameters are presented in Figure S6.

The INT structure has been obtained through inter-strand flipping of the UBP in the EXT conformer (Figure 4). For the INT_{SYN} conformer, the intercalation of DS-DN was also maintained during the entire simulation with both force fields, with low RMSD value (average RMSD for each replicate > 2.6 Å for AMBER) (Table 1 and Figure S2). RMSF values obtained from the AMBER simulated system indicates that the fluctuation of all the residues including UBP are low. Similar to EXT_{SYN} , the INT_{SYN} system exhibits no conformational change and no significant distortion, suggesting that in this case the flexibility of the UBP has also been prevented by *Taq*. It is also evident (Figure 3) that along with most of the protein-DNA

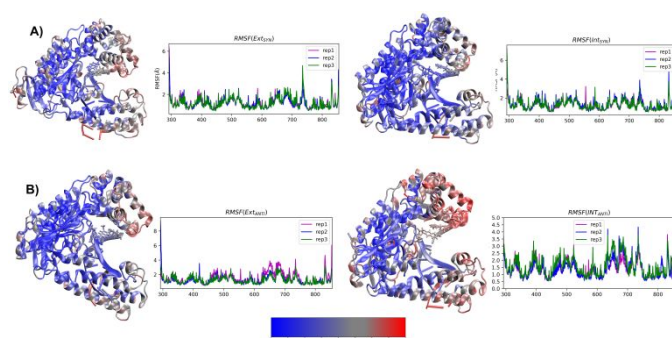


Figure 3. 3D representations of average RMSF values of the protein-DNA residues and associated RMSF plots of three replicates of EXT and INT structures; A) SYN and B) ANTI conformers obtained from AMBER simulations.

residues, DS and DN also display low RMSF values confirming the relatively low fluctuating nature of the UBP.

The pattern of fluctuations of the polymerase residues as observed from the RMSF analysis is similar to EXT_{SYN} , suggesting that a conformational change of the UBP doesn't influence the characteristics of the system. In this case also the calculated $d_{\text{DS-DN}}$ distance, derived from both AMOEBA and AMBER force fields, is found to be lower than that of nBPs. Asymmetry of the DNA duplex is reflected in the associated uneven $d_{\text{UB-NB}}$ (Figure 2) and $\langle \text{UB-P-NB} \rangle$ (Figure S4) obtained from both AMOEBA and AMBER simulations. It is observed that here $d_{\text{DS-DC}}$ and $\langle \text{DS-P-DC} \rangle$ are found to be lower than $d_{\text{DN-DG}}$ and $\langle \text{DN-P-DG} \rangle$ respectively, which is in agreement with the crystal structure. Comparing these geometrical parameters between EXT_{SYN} and INT_{SYN} , contrasting trajectories have been observed from which two conformers can be distinguished. Here also there is no significant deviations between the AMBER and AMOEBA results as both predict similar structural behaviour. We have further simulated no-overhang INT_{SYN} system with the AMBER force field from which it is evident that in absence of hanging base pair also UBP can stabilize an

intercalated structure with low RMSD values and similar RMSF and geometrical parameters (Figure S5). It also suggests that hanging base pair has no significant influence on the formation of nWCF UBP-incorporated DNA strand in *Taq*.

Despite the conformational dissimilarities between EXT_{SYN} and INT_{SYN} , they exhibit mostly similar RMSF pattern ($\Delta RMSF \sim 0$). (Figure S5) This is further supported by the cross-correlation analyses for both systems (Figure S8), which demonstrates similar correlation patterns among the residues for both EXT_{SYN} and INT_{SYN} . Normal mode analysis also indicates that exclusive dominance of the 1st normal mode has been observed with similar vibration pattern (supporting information).

To investigate the effect of conformational change on *Taq*, we have generated the EXT_{ANTI} system via an intra-strand flipping of the DS in the EXT_{SYN} structure where the sulfur of DS and methoxy group of DN are on opposite sides. As discussed in

our previous article⁵¹, the UBP can stay in both SYN and ANTI forms within DNA in aqueous solution with spontaneous intra-strand flipping. As depicted in Figure 5, O-S distance for INT_{SYN} is lower than INT_{ANTI} . But simulations of UBP-intercalated DNA bound to *Taq* suggests that the EXT_{ANTI} conformer of UBP inside the DNA duplex is disfavored, leading to a non-pairing between DS and DN inside the DNA duplex (Figure 1). From all three replicates it has been found that DS-DN fails to generate an intercalated structure, and rather DS is flanked out from the DNA duplex. Comparatively higher RMSD value (Figure 2) suggests that EXT_{ANTI} induces larger structural changes compared with the SYN conformation. Notably, some specific polymerase residues mainly from the finger region of the polymerase exhibit higher RMSF ($\Delta RMSF_{(SYN-ANTI)} > 0$) values (Figure S5). From cross-correlation analysis also, significant deviation of movement correlation among the polymerase residues has been observed between SYN and ANTI conformation (Figure S8).

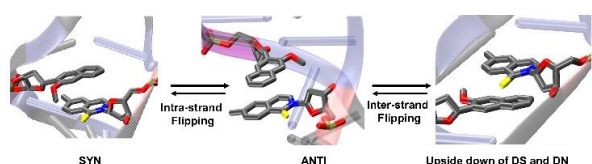


Figure 4. Conformational change through Intra- and Inter-strand flipping observed during the MD simulations. (Figure taken from preprint with permission⁵¹).

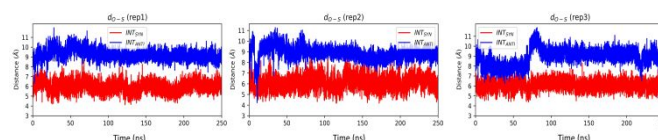


Figure 5. O-S distance for INT_{SYN} and INT_{ANTI} conformers obtained from AMBER simulation. O-S distance of crystal structure of INT_{SYN} is 7.4 Å. Distance value are in Å.

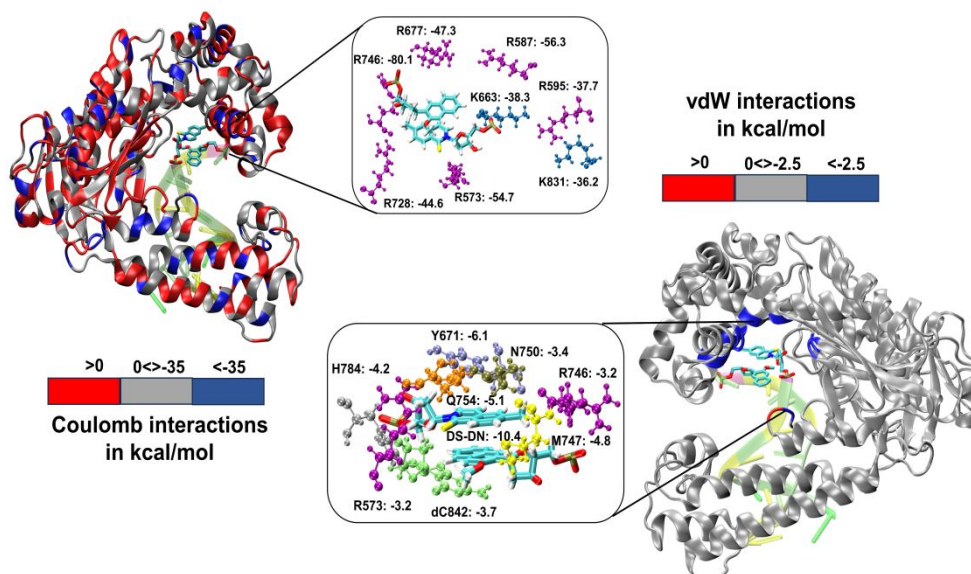


Figure 6. 3D representation of non-covalent interactions between polymerase residues and UBP through EDA for Ext_{SYN} . Residues with Coulomb interactions < -35.0 kcal/mol and vdW interactions < -2.5 kcal/mol are highlighted. Energy values are in kcal/mol.

INT_{SYN} is further reoriented through intra-strand flipping the DS which leads to the production of INT_{ANTI} structure (Figure 1). Despite the conformational change, this UBP conformation results in an intercalated structure in *Taq* with similar pattern of average RMSD value throughout the simulation (Figure 2). RMSF analysis suggests that apart from terminal residues, the fluctuation of most polymerase residues is below 4.5 Å, indicating low degree of flexibility. Here also it is observed

negative E_{Coul} for all the conformers but only reported for EXT_{SYN} from crystal structure analysis. These findings lead to create a scope to extend the experimental investigation through mutagenesis techniques to identify the *Taq* residues that interact with UBP in different conformers. EDA also predicts that residues residing in the finger region of *Taq* interacting with the UBP through vdW interactions. Tyr671 is known as the steric gate, which is crucial for rNTP

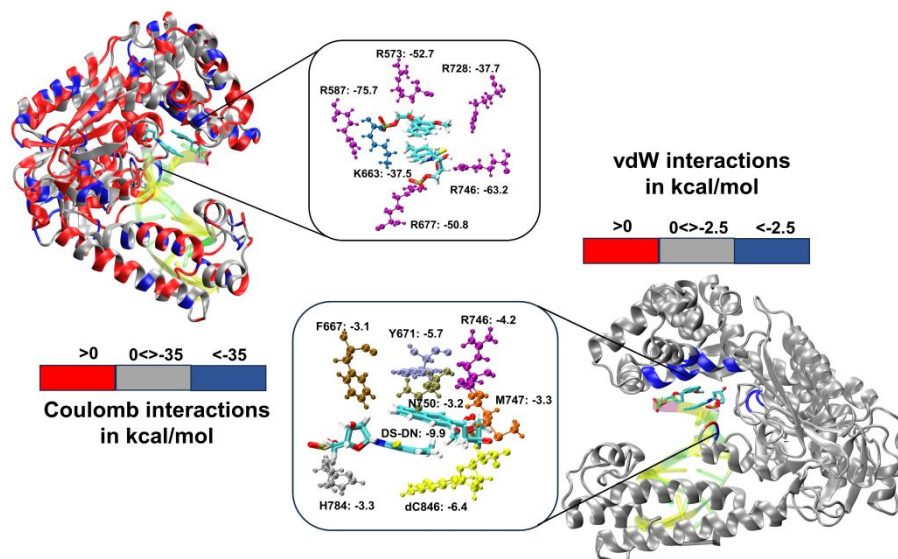


Figure 7. Non-covalent interactions between polymerase residues and for Int_{SYN}. Residues with Coulomb interactions < -35.0 kcal/mol and vdW interactions < -2.5 kcal/mol are highlighted. Energy values are in kcal/mol.

that for ANTI conformer, polymerase residues from finger region fluctuate more compared to SYN indicating perturbation arises on conformational change on the finger region. Average DS-DN distance is found to be ~ 9.1 Å, indicating minor reduction of the distance as obtained from SYN conformer (Figure 2). The persistence of intercalated geometry of the UBP suggests that, unlike EXT, the INT conformer doesn't result in mispairing through intra-strand flipping, indicating that both SYN and ANTI orientations are tolerated by *Taq* for INT UB conformers.

We have further performed EDA analysis to identify and quantify individual interactions between individual protein residues and the UBP (Figures S9-S10). It has been observed that attractive Coulomb interactions (E_{Coul}) arise mostly from positively charged residues. Arg and Lys, from all three polymerase subdomains (Figures 6-7). For all the conformers, R587 and R746 exhibit the highest E_{Coul} with the UBP through interactions with the phosphate backbone of 3'-DS and 5'-DN respectively. Interestingly, these two residues are identified in the interacting zone with the phosphate backbone of DS and DN from the crystal structure analysis of 4C8L (EXT_{SYN}) but not for 4C80 (INT_{SYN}) by Romesberg *et al.* R573 is also found to be strongly interacting with the UBs having higher

discrimination. Interestingly, in the case of UBPs, Tyr671 exhibits stabilizing vdW interactions with the exposed UBs (DS for EXT_{SYN} and DN for INT_{SYN}) which is also in agreement with the findings from crystal structure analysis. Nevertheless, a disparity between experimental observations and our EDA results becomes evident concerning Glu615. While crystal structure analysis propose that Glu615 forms attractive interactions with DS, our EDA findings indicate that while the van der Waals interaction is indeed attractive, the Coulombic interaction is significantly repulsive in nature and consequently the total non-covalent interaction energy between DS and Glu615 becomes positive. This is consistent with the fact that Glu615, being a negatively charged residue in physiological pH exhibits repulsive Coulombic interactions with the phosphate backbone of the UBP.

Comparing the EDA results of *Taq*-UBP-incorporated DNA with the 3.2 Å resolution mapped structures of *Taq*-nB-DNA⁸³ it is observed that interaction profile (E_{vdW}) looks mostly similar for both the cases. A notable distinction observed is that, in the case of nBP, Tyr671 and Phe667 form interactions with the 5'- and 3'-BP positions, respectively. In contrast,

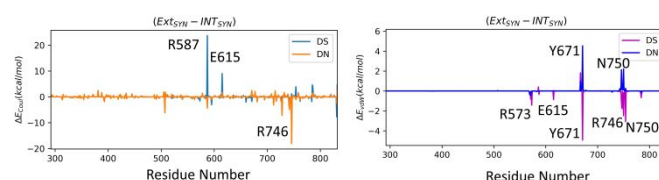


Figure 8. Difference in interaction profiles (ΔE_{Coul} and ΔE_{vdW}) between EXT_{SYN} and INT_{SYN}. Energy values are in kcal/mol.

when the UBP is incorporated into DNA, significant interactions primarily occur between the exposed UBs (3'-DS for EXT_{SYN} and 5'-DN INT_{SYN}) and Tyr671. Additionally, in the INT_{SYN} scenario, instead of the Phe667-5'-BP interaction, we observed E_{vdW} interaction between Phe667 and the 3'-DS.

We have further calculated the total inter-molecular interaction (interaction between UBP and sum of all the *Taq* residues) differences (ΔE_{Tot}) between different conformers. The difference in total interaction energy ΔE_{Tot} between EXT_{SYN} and INT_{SYN} is found to be insignificant (-3.5 kcal/mol) suggesting the similar stability of the UBP inside *Taq* for both of these conformers. However, EXT_{ANTI} displays a significant increase of ΔE_{Tot} as compared to EXT_{SYN} ($\Delta E_{\text{Tot}} = 70.4$ kcal/mol) implying intra-strand flipping is not favored for EXT conformer, which is consistent with this conformation not being structurally stabilized. For INT, ΔE_{Tot} between SYN and ANTI is found to be -12.4 kcal/mol indicating despite energetic difference INT_{ANTI} is also significantly stabilized inside *Taq*.

Mutation of R660S of the homologous *E. coli* DNA polymerase I (Klenow fragment, KF) conducted by Yosida et al. revealed a reduction in transitions from T to C.⁸⁴ Thompson et al. reported changes in fidelity by mutating 26 amino acids in the KF, and found that DNA mismatches are recognized by two important factors; free energy difference for the partitioning of the DNA primer terminus i) between the polymerase and exonuclease sites for several mispairs, ii) between the residues near the active site and the mismatched pairs.⁴⁶ They concluded that residues N845 and R668 are required for recognition of correct mispairs. Singh and Modak also reported that residues N845, Q849, R668, H881, and Q677 are part of a hydrogen bond track. Computational studies have also been done to investigate the effect of mutation of DNA polymerase I towards mispairing of the base pairs in the terminal positions.^{49,85}

Collectively, previous studies confirmed that mutation of KF residues R668, R682, E710 and N845 (R573, R587, E615 and Asn750 for *Taq*) are the key residues controlling the fidelity within the KF⁸⁴⁻⁸⁷ whereas E742 and A743 are found to be crucial for the elongation activity⁸⁷. Our studies also identified similar residues with significant interactions (E) with UBP particularly for EXT_{SYN}, INT_{SYN} and INT_{ANTI}. Interestingly these residues also exhibit significant difference in interactions (ΔE) on conformational change. It has been observed that Coulomb interaction profile (E_{Coul}) almost looks similar apart from few residues (R573, R587, E615 and R746) displaying significant altered interactions ($\Delta E_{\text{Coul}} \neq 0$) from EXT_{SYN} to INT_{SYN}. (Figure 8) Similar vdW interaction profile (E_{vdW}) has also been

observed for these two conformers with few residues exhibiting altered vdW interactions ($\Delta E_{\text{vdW}} \neq 0$) on finger region. Intra-strand flipping between SYN and ANTI also leads to minimal perturbation of Coulomb and vdW interaction between UBP and *Taq* (Figure 9). The difference in inter-molecular interactions between the different UBP orientations results in almost all residues exhibiting similar (de)stabilizing roles, albeit there are some exceptions, among them R573, R587, E615, E742 and R746 are significant. However, the difference of interaction profile is prominent

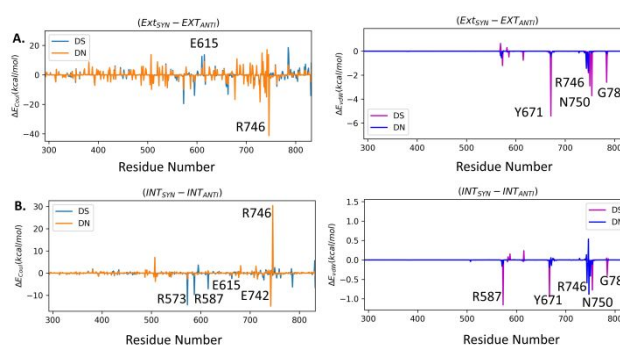


Figure 9. Difference in interaction profiles (ΔE_{Coul} and ΔE_{vdW}) between A) EXT_{SYN} and EXT_{ANTI}, B) INT_{SYN} and INT_{ANTI}. Energy values are in kcal/mol.

between SYN and ANTI for EXT with several residues showing altered interactions indicating the EXT_{ANTI} is not stabilized by *Taq*, leading to non-pairing of the UBP. The extent of non-covalent interactions between DS and DN is also obtained from EDA. Interaction between DS and DN is found to be highest for EXT_{SYN} ($E_{\text{vdW}} = -10.4$ kcal/mol) followed by INT_{SYN} ($E_{\text{vdW}} = -9.9$ kcal/mol) and INT_{ANTI} ($E_{\text{vdW}} = -9.2$ kcal/mol) and least for EXT_{ANTI} ($E_{\text{vdW}} = -3.5$ kcal/mol) indicating apart from EXT_{ANTI} intercalation persist for all three conformers. During the examination of adjacent nBP interactions, EDA analysis indicates that the neighboring base pair exhibits relatively lower stability when contrasted with other base pairs, which suggest that the structure and stability of adjacent BP have been affected by the presence of the unconventional orientation of UBP.

Conclusions

Our research delved into the structural characteristics and conformational orientations of UBP-incorporated DNA within the binary *Taq*. Further, we conducted an in-depth analysis to predict the interaction profile between UBP and *Taq* through Coulombic and vdW interactions. Both the AMOEBA and AMBER force fields employed in this study produce consistent results that agree with experimental outcomes. Our simulated

results predict that flexibility of the UBP- incorporated DNA, observed in the solution, is arrested by the polymerase. This stabilization leads to a stable intercalated form of the UBP that is conducive to DNA polymerization with unnatural bases. It has been observed that inter-strand flipping from EXT to INT leads to the generation of minimal perturbation of the stabilization of the UBP within *Taq*, whereas intra-strand flipping from SYN to ANTI leads to the generation of a non-pairing structure of the UBP with significant perturbations in the polymerase residues specifically for EXT conformers. Further EDA analysis established the interaction profiles between UBP and polymerase residues which also depicts minor differences of interactions during inter-strand flipping and intra-strand flipping for INT. Lack of pairing of DS-DN in EXT_{ANTI} leads to change the interaction profiles significantly. Unlike nBP-polymerase interactions, Tyr671 interacts with both 3' and 5'-UB depending on the exposure of the UB in the conformers. Overall, our systematic MD simulation associated with EDA analysis portrayed the structural properties, effect of conformational changes and interaction profiles of binary system of *Taq* in complex with a DNA duplex including an intercalated DS-DN pair.

AUTHOR INFORMATION

Corresponding Author

G. Andrés Cisneros—Department of Physics, The University of Texas at Dallas, Richardson, Texas 75080, United States; Department of Physics, The University of Texas at Dallas, Richardson, Texas 75080, United States; orcid.org/0000-0001-6629-3430; Email: andres@utdallas.edu

Author

Tanay Debnath—Department of Physics, The University of Texas at Dallas, Richardson, Texas 75080, United States; orcid.org/0000-0001-8672-1834

Funding Information

This work was supported by R01GM108583 and Fulbright-Nehru postdoctoral Scholarship. Computing time from UNT CASCaM funded by NSF Grant Nos. CHE1531468 and OAC-2117247 is gratefully acknowledged.

ACKNOWLEDGMENT

Tanay Debnath is a USIEF postdoctoral fellow (Fulbright-Nehru postdoctoral Scholarship). Computational time for this project was provided by the University of North Texas CASCaM CRUNTCh3 and 4 high-performance cluster and the University of

Texas at Dallas, Cyberinfrastructure and Research Services, Ganymede and Titan HPC clusters and NCSA DELTA at University of Illinois Urbana-Champaign. The authors thank the reviewers for their constructive comments, which have helped improve our manuscript.

Conflicts of interest

“There are no conflicts to declare”.

References

- [1] J. D. Watson and F. H. C. Crick, *Nature* **1953**, *171*, 737-738.
- [2] P. S. Freemont, J. M. Friedman, L. S. Beese, M. R. Sanderson and T. A. Steitz, *Proceedings of the National Academy of Sciences* **1988**, *85*, 8924-8928.
- [3] L. S. Beese, J. M. Friedman and T. A. Steitz, *Biochemistry* **1993**, *32*, 14095-14101.
- [4] R. D. Kuchta, P. Benkovic and S. J. Benkovic, *Biochemistry* **1988**, *27*, 6716-6725.
- [5] K. Singh and M. J. Modak, *Biochemistry* **2005**, *44*, 8101-8110.
- [6] J. Gouge, C. Ralec, G. Henneke and M. Delarue, *Journal of Molecular Biology* **2012**, *423*, 315-336.
- [7] K. H. Lee, K. Hamashima, M. Kimoto and I. Hirao, *Current Opinion in Biotechnology* **2018**, *51*, 8-15.
- [8] D. A. Malyshev and F. E. Romesberg, *Angewandte Chemie International Edition* **2015**, *54*, 11930-11944.
- [9] S. Hoshika, N. A. Leal, M.-J. Kim, M.-S. Kim, N. B. Karalkar, H.-J. Kim, A. M. Bates, N. E. Watkins, H. A. SantaLucia, A. J. Meyer, S. DasGupta, J. A. Piccirilli, A. D. Ellington, J. SantaLucia, M. M. Georgiadis and S. A. Benner, *Science* **2019**, *363*, 884-887.
- [10] T. P. Hettinger, *Proceedings of the National Academy of Sciences* **2017**, *114*, E6476-E6477.
- [11] R. Yamashige, M. Kimoto, Y. Takezawa, A. Sato, T. Mitsui, S. Yokoyama and I. Hirao, *Nucleic Acids Research* **2012**, *40*, 2793-2806.
- [12] M. Manandhar, E. Chun and F. E. Romesberg, *Journal of the American Chemical Society* **2021**, *143*, 4859-4878.
- [13] D. A. Malyshev, K. Dhami, H. T. Quach, T. Lavergne, P. Ordoukhanian, A. Torkamani and F. E. Romesberg, *Proceedings of the National Academy of Sciences* **2012**, *109*, 12005-12010.
- [14] K. Hashimoto, E. C. Fischer and F. E. Romesberg, *Journal of the American Chemical Society* **2021**, *143*, 8603-8607.
- [15] N. Tarashima, Y. Komatsu, K. Furukawa and N. Minakawa, *Chemistry (Weinheim an der Bergstrasse, Germany)* **2015**, *21*, 10688-10695.
- [16] M. Kimoto, R. Yamashige, K.-i. Matsunaga, S. Yokoyama and I. Hirao, *Nature Biotechnology* **2013**, *31*, 453-457.
- [17] N. R. Jena and P. Das, *Journal of Biomolecular Structure and Dynamics* **2023**, *41*, 366-376.
- [18] N. Beiranvand, M. Freindorf and E. Kraka in *Hydrogen Bonding in Natural and Unnatural Base Pairs—A Local Vibrational Mode Study, Vol. 26* **2021**.
- [19] J. Riedl, Y. Ding, A. M. Fleming and C. J. Burrows, *Nature Communications* **2015**, *6*, 8807.
- [20] M. M. Georgiadis, I. Singh, W. F. Kellett, S. Hoshika, S. A. Benner and N. G. J. Richards, *Journal of the American Chemical Society* **2015**, *137*, 6947-6955.

- [21] R. Dörrenhaus, P. K. Wagner and S. Kath-Schorr, **2023**.
- [22] M. Kimoto and I. Hirao, *ACS Synthetic Biology* **2017**, *6*, 1944-1951.
- [23] I. Hirao and M. Kimoto, *Proceedings of the Japan Academy, Series B* **2012**, *88*, 345-367.
- [24] T. Lavergne, D. A. Malyshev and F. E. Romesberg, *Chemistry – A European Journal* **2012**, *18*, 1231-1239.
- [25] S. Ochoa and V. T. Milam in *Modified Nucleic Acids: Expanding the Capabilities of Functional Oligonucleotides*, Vol. 25 **2020**.
- [26] A. Ambrogelly, S. Palioura and D. Söll, *Nature Chemical Biology* **2007**, *3*, 29-35.
- [27] I. Hirao, M. Kimoto and R. Yamashige, *Accounts of Chemical Research* **2012**, *45*, 2055-2065.
- [28] M. P. Ledbetter, R. J. Karadeema and F. E. Romesberg, *Journal of the American Chemical Society* **2018**, *140*, 758-765.
- [29] C. Kaul, M. Müller, M. Wagner, S. Schneider and T. Carell, *Nature Chemistry* **2011**, *3*, 794-800.
- [30] K. Betz, D. A. Malyshev, T. Lavergne, W. Welte, K. Diederichs, T. J. Dwyer, P. Ordoukhanian, F. E. Romesberg and A. Marx, *Nature Chemical Biology* **2012**, *8*, 612-614.
- [31] K. Betz, D. A. Malyshev, T. Lavergne, W. Welte, K. Diederichs, F. E. Romesberg and A. Marx, *Journal of the American Chemical Society* **2013**, *135*, 18637-18643.
- [32] A. Marx and K. Betz, *Chemistry – A European Journal* **2020**, *26*, 3446-3463.
- [33] D. A. Malyshev, K. Dhami, T. Lavergne, T. Chen, N. Dai, J. M. Foster, I. R. Corrêa and F. E. Romesberg, *Nature* **2014**, *509*, 385-388.
- [34] F. E. Romesberg in *Unnatural Base Pairs to Expand the Genetic Alphabet and Code*, (Ed. N. Sugimoto), Springer Nature Singapore, Singapore, **2022**, pp. 1-21.
- [35] A. W. Feldman, V. T. Dien, R. J. Karadeema, E. C. Fischer, Y. You, B. A. Anderson, R. Krishnamurthy, J. S. Chen, L. Li and F. E. Romesberg, *Journal of the American Chemical Society* **2019**, *141*, 10644-10653.
- [36] L. Sun, X. Ma, B. Zhang, Y. Qin, J. Ma, Y. Du and T. Chen, *RSC Chemical Biology* **2022**, *3*, 1173-1197.
- [37] A. W. Feldman and F. E. Romesberg, *Accounts of Chemical Research* **2018**, *51*, 394-403.
- [38] A. W. Feldman and F. E. Romesberg, *Journal of the American Chemical Society* **2017**, *139*, 11427-11433.
- [39] M. Kimoto and I. Hirao, *Chemical Society Reviews* **2020**, *49*, 7602-7626.
- [40] E. C. Fischer, K. Hashimoto, Y. Zhang, A. W. Feldman, V. T. Dien, R. J. Karadeema, R. Adhikary, M. P. Ledbetter, R. Krishnamurthy and F. E. Romesberg, *Nature Chemical Biology* **2020**, *16*, 570-576.
- [41] J. Oh, J. Shin, I. C. Unarta, W. Wang, A. W. Feldman, R. J. Karadeema, L. Xu, J. Xu, J. Chong, R. Krishnamurthy, X. Huang, F. E. Romesberg and D. Wang, *Nature Chemical Biology* **2021**, *17*, 906-914.
- [42] S. A. Mukba, P. K. Vlasov, P. M. Kolosov, E. Y. Shuvalova, T. V. Egorova and E. Z. Alkalaeva, *Molecular Biology* **2020**, *54*, 475-484.
- [43] T. D. Christian, L. J. Romano and D. Rueda, *Proceedings of the National Academy of Sciences* **2009**, *106*, 21109-21114.
- [44] V. Khare and K. A. Eckert, *Mutation Research/Fundamental and Molecular Mechanisms of Mutagenesis* **2002**, *510*, 45-54.
- [45] K. A. Johnson, *Biochimica et Biophysica Acta (BBA) - Proteins and Proteomics* **2010**, *1804*, 1041-1048.
- [46] E. H. Z. Thompson, M. F. Bailey, E. J. C. van der Schans, C. M. Joyce and D. P. Millar, *Biochemistry* **2002**, *41*, 713-722.
- [47] S. K. Jozwiakowski, B. J. Keith, L. Gilroy, A. J. Doherty and B. A. Connolly, *Nucleic Acids Research* **2014**, *42*, 9949-9963.
- [48] A. R. Walker and G. A. Cisneros, *Chemical Research in Toxicology* **2017**, *30*, 1922-1935.
- [49] A. A. Elias and G. A. Cisneros, *Adv Protein Chem Struct Biol* **2014**, *96*, 39-75.
- [50] L. Aravind and E. V. Koonin, *Nucleic Acids Research* **1998**, *26*, 3746-3752.
- [51] G. A. C. Tanay Debnath.
- [52] I. Negi, P. Kathuria, P. Sharma and S. D. Wetmore, *Physical Chemistry Chemical Physics* **2017**, *19*, 16365-16374.
- [53] R. Galindo-Murillo and J. Barroso-Flores, *Physical Chemistry Chemical Physics* **2017**, *19*, 10571-10580.
- [54] R. Galindo-Murillo and J. Barroso-Flores, *Journal of Biomolecular Structure and Dynamics* **2020**, *38*, 4098-4106.
- [55] L. Eberlein, F. R. Beierlein, N. J. R. van Eikema Hommes, A. Radadiya, J. Heil, S. A. Benner, T. Clark, S. M. Kast and N. G. J. Richards, *Journal of Chemical Theory and Computation* **2020**, *16*, 2766-2777.
- [56] S. Jahiruddin and A. Datta, *The Journal of Physical Chemistry B* **2015**, *119*, 5839-5845.
- [57] S. Jahiruddin, N. Mandal and A. Datta, *ChemPhysChem* **2018**, *19*, 67-74.
- [58] H. Wang, L. Wang, N. Ma, W. Zhu, B. Huo, A. Zhu and L. Li, *ACS Synthetic Biology* **2022**, *11*, 334-342.
- [59] <https://upjv.q4md-forcefieldtools.org/REDServer-Development/overview.php>.
- [60] P. Mark and L. Nilsson, *The Journal of Physical Chemistry A* **2001**, *105*, 9954-9960.
- [61] C. Tian, K. Kasavajhala, K. A. A. Belfon, L. Raguette, H. Huang, A. N. Miguez, J. Bickel, Y. Wang, J. Pincay, Q. Wu and C. Simmerling, *Journal of Chemical Theory and Computation* **2020**, *16*, 528-552.
- [62] M. Zgarbová, J. Šponer, M. Otyepka, T. E. Cheatham, III, R. Galindo-Murillo and P. Jurečka, *Journal of Chemical Theory and Computation* **2015**, *11*, 5723-5736.
- [63] P. Ren and J. W. Ponder, *Journal of Computational Chemistry* **2002**, *23*, 1497-1506.
- [64] P. Ren and J. W. Ponder, *The Journal of Physical Chemistry B* **2003**, *107*, 5933-5947.
- [65] P. Ren and J. W. Ponder, *The Journal of Physical Chemistry B* **2004**, *108*, 13427-13437.
- [66] P. Ren, C. Wu and J. W. Ponder, *Journal of Chemical Theory and Computation* **2011**, *7*, 3143-3161.
- [67] L. Lagardère, L.-H. Jolly, F. Lipparini, F. Aviat, B. Stamm, Z. F. Jing, M. Harger, H. Torabifard, G. A. Cisneros, M. J. Schnieders, N. Gresh, Y. Maday, P. Y. Ren, J. W. Ponder and J.-P. Piquemal, *Chemical Science* **2018**, *9*, 956-972.
- [68] A. J. Stone, *Journal of Chemical Theory and Computation* **2005**, *1*, 1128-1132.

- [69] C. Schafmeister, W. Ross and V. J. G. S. T. i. n. c. r. f. t. r. Romanovski. LEAP; University of California: San Francisco, 1995.
- [70] D.A. Case, K. Belfon, I.Y. Ben-Shalom, S.R. Brozell, D.S. Cerutti, T.E. Cheatham, III, V.W.D. Cruzeiro, T.A. Darden, R.E. Duke, G. Giambasu, M.K. Gilson, H. Gohlke, A.W. Goetz, R. Harris, S. Izadi, S.A. Izmailov, K. Kasavajhala, A. Kovalenko, R. Krasny, T. Kurtzman, T.S. Lee, S. LeGrand, P. Li, C. Lin, J. Liu, T. Luchko, R. Luo, V. Man, K.M. Merz, Y. Miao, O. Mikhailovskii, G. Monard, H. Nguyen, A. Onufriev, F. Pan, S. Pantano, R. Qi, D.R. Roe, A. Roitberg, C. Sagui, S. Schott-Verdugo, J. Shen, C.L. Simmerling, N.R. Skrynnikov, J. Smith, J. Swails, R.C. Walker, J. Wang, L. Wilson, R.M. Wolf, X. Wu, Y. Xiong, Y. Xue, D.M. York and P.A. Kollman (2020), AMBER 2020, University of California, San Francisco.
- [71] M. H. M. Olsson, C. R. Søndergaard, M. Rostkowski and J. H. Jensen, *Journal of Chemical Theory and Computation* **2011**, 7, 525-537.
- [72] C. R. Søndergaard, M. H. M. Olsson, M. Rostkowski and J. H. Jensen, *Journal of Chemical Theory and Computation* **2011**, 7, 2284-2295.
- [73] J.-P. Ryckaert, G. Ciccotti and H. J. C. Berendsen, *Journal of Computational Physics* **1977**, 23, 327-341.
- [74] R. Salomon-Ferrer, A. W. Götz, D. Poole, S. Le Grand and R. C. Walker, *Journal of Chemical Theory and Computation* **2013**, 9, 3878-3888.
- [75] D. R. Roe and T. E. Cheatham, III, *Journal of Chemical Theory and Computation* **2013**, 9, 3084-3095.
- [76] S. v. d. Walt, S. C. Colbert and G. Varoquaux, *Computing in Science & Engineering* **2011**, 13, 22-30.
- [77] J. D. Hunter, *Computing in Science & Engineering* **2007**, 9, 90-95.
- [78] W. McKinney, In Data Structures for Statistical Computing in Python, Proceedings of the 9th Python in Science Conference, Austin, TX, **2010**, Vol. 445, p. 51-56.
- [79] Emmett Leddin, Cisneros Research Group, & G. Andres Cisneros. (2021). CisnerosResearch/AMBER-EDA: First Release (v0.1). Zenodo. <https://zenodo.org/records/4469902>.
- [80] L. Martínez, R. Andrade, E. G. Birgin and J. M. Martínez, *Journal of Computational Chemistry* **2009**, 30, 2157-2164.
- [81] U. Essmann, L. Perera, M. L. Berkowitz, T. Darden, H. Lee and L. G. Pedersen, *The Journal of Chemical Physics* **1995**, 103, 8577-8593.
- [82] P. J. Steinbach and B. R. Brooks, **1994**, 15, 667-683.
- [83] S. H. Eom, J. Wang and T. A. Steitz, *Nature* **1996**, 382, 278-281.
- [84] K. Yoshida, A. Tosaka, H. Kamiya, T. Murate, H. Kasai, Y. Nimura, M. Ogawa, S. Yoshida and M. Suzuki, *Nucleic Acids Research* **2001**, 29, 4206-4214.
- [85] K. Singh and M. J. Modak, *Journal of Biological Chemistry* **2003**, 278, 11289-11302.
- [86] S. E. Graham, F. Syeda and G. A. Cisneros, *Biochemistry* **2012**, 51, 2569-2578.
- [87] T. Yamagami, S. Ishino, Y. Kawarabayasi and Y. Ishino, **2014**, 5.